EPJ Web of Conferences **17**, 13003 (2011)
DOI: 10.1051/epjconf/20111713003

Fusion reactions with the one-neutron halo nucleus ^{15}C

M. Alcorta[1,a], K. E. Rehm[1], B. B. Back[1], S. Bedoor[2], P. F. Bertone[1], C. M. Deibel[1,3], B. DiGiovine[1], H. Esbensen[1], J. P. Greene[1], C. R. Hoffman[1], C. L. Jiang[1], J. C. Lighthall[1,2], S. T. Marley[1,2], R. C. Pardo[1], M. Paul[4], A. M. Rogers[1], C. Ugalde[1,5,6], and A. H. Wuosmaa[2]

[1] Physics Division, Argonne National Laboratory, Argonne, IL 60439, USA
[2] Western Michigan University, Kalamazoo, MI 49008, USA
[3] Joint Institute for Nuclear Astrophysics, Michigan State University, East Lansing, MI 48824, USA
[4] Racah Institute of Physics, Hebrew University, Jerusalem, 91904, Israel
[5] Department of Astronomy and Astrophysics, University of Chicago, Chicago, IL 60637 USA
[6] Joint Institute for Nuclear Astrophysics, Chicago, IL 60637 USA

Abstract. We have for the first time studied the fusion-fission excitation functions for the systems ^{14,15}C + ^{232}Th at energies in the vicinity of the Coulomb barrier. At energies below the barrier, the fusion cross section of the halo nucleus ^{15}C showed an enhancement by a factor of 2-5, while the fusion cross section for ^{14}C shows a similar trend to that of ^{12,13}C.

1 Introduction

There has been a strong interest in reaction studies involving so-called halo nuclei since their anomalously large interaction radii were discovered more than 25 years ago [1]. The definition of a halo nucleus is still being debated, but at least three conditions are required [2]: (i) low separation energy of the valence particle (or particle cluster); (ii) a wave function that is in a low relative angular momentum state (preferably an s-wave); (iii) decoupling from the core. The nucleus ^{11}Li, a two-neutron halo nucleus, is a prime example.

Possible candidates for one-neutron halo nuclei are still being debated. For example, in Ref. [2] ^{11}Be, ^{15}C, ^{19}C and ^{23}O are listed as candidates, based mainly on the width of their momentum distributions measured in one-neutron removal reactions [3]. The latter two isotopes are located far away from the valley of stability and are currently not available with beam intensities sufficient to allow for studies of fusion reactions. The remaining two nuclei, ^{11}Be and ^{15}C, are closer to the valley of β stability and can be produced with higher beam intensities. Measurements of interaction radii for ^{11}Be and ^{15}C at a high bombarding energy of 950 MeV/u [4] showed a radius increase only for ^{11}Be. Later studies at lower energies (E~83 and 51 MeV/u) [5], however, demonstrated an increase in the interaction radius of ^{15}C when compared to those of the neighboring ^{14,16}C isotopes.

The ground state of ^{15}C can be described as an $s_{1/2}$ neutron coupled to a ^{14}C core with a separation energy of 1.218 MeV and a spectroscopic factor of ~1 as measured in the ^{14}C(d,p)^{15}C reaction [6]. In comparison, ^{11}Be has a smaller neutron separation energy (0.503 MeV), but a slightly smaller one-neutron spectroscopic factor (see Ref. [7] and references quoted therein). Several fusion experiments with ^{11}Be beams have been performed [8–10]. Their interpretation suffers from the difficulty of not having a good spherical nucleus as a reference system. Early experiments used ^{9}Be [10], which also has a low neutron binding energy of 1.665 MeV. Later studies replaced ^{9}Be with the even-even nucleus ^{10}Be, yet no enhancement in the fusion cross sections was found in either case.

For the nucleus ^{17}F, in which the first excited state is a proton halo, no fusion enhancement was observed experimentally [11]. This observation was explained through the polarization of the incoming ^{17}F projectile in the Coulomb field of the ^{208}Pb target nucleus, which keeps the weakly-bound proton away from the interaction zone. However, there is at present no consensus on the behavior of the low-energy fusion cross sections induced by halo nuclei. Reviews on this topic have been published in Refs. [12–15], and several theoretical predictions can be found in the literature [16–20]. These calculations include coupling to soft dipole modes and to transfer and breakup channels. Both enhancement and suppression of the fusion cross sections at low energies has been predicted.

2 Experiment

We have measured the fusion-fission cross sections in the systems ^{13,14,15}C + ^{232}Th at energies in the vicinity of the Coulomb barrier [21]. The ^{13}C + ^{232}Th excitation function was measured first and was used to determine the detection efficiency by normalizing the data to the results from Ref. [22]. The next step was to measure the excitation function for the system ^{14}C + ^{232}Th. This provided a closed

[a] e-mail: malcorta@anl.gov

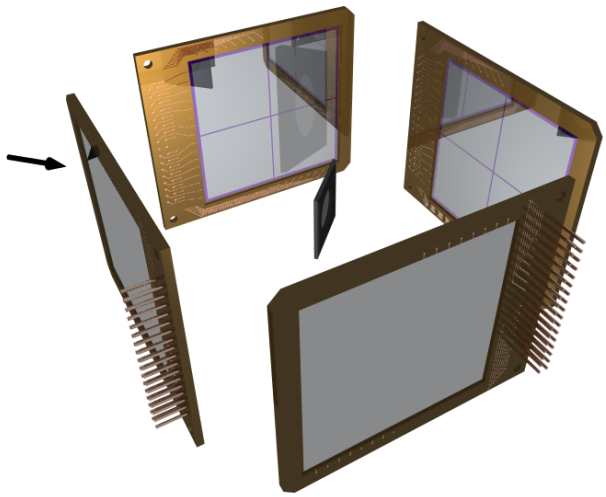

Fig. 1. Experimental setup. The front side of each detector was divided into four quadrants. The detectors were each located ~6 cm from the target.

shell nuclei (S_n=8.177 MeV) as a reference measurement involving a spherical projectile. Finally, the measurement involving the excitation function of the halo nucleus ^{15}C + ^{232}Th was performed.

2.1 Experimental setup

The experimental setup is displayed in Fig. 1. It consists of four 5x5 cm^2 Si surface barrier detectors subdivided into four quadrants surrounding the self-supporting ^{232}Th target (640 μg/cm^2). Two pairs of Si detectors are located at 180° relative to each other, and the total angular range covered by the detector pairs is 25° – 70° and 115° – 160°. The fusion-fission events were identified by detecting two high-energy particles in opposite detectors in coincidence. At a distance of 6 cm from the target, the four detectors provided an average detection efficiency of 5.1% as calculated by a Monte Carlo simulation. However, in order to be independent of the calculated efficiency which depends on the angle between the two fission fragments, the detection efficiency was extracted by normalizing the measured ^{13}C + ^{232}Th fusion-fission yields to the data from Ref. [22]. This gave a detection efficiency of 5.3%, in good agreement with the Monte Carlo simulation.

The beam energy changes for the measurements of the fusion excitation function were achieved by using Au degrader foils with thicknesses ranging from 4.9 to 14.9 mg/cm^2. These degrader foils were inserted into the beam ~55 cm upstream from the target, causing a reduction in beam intensity by factors of 3-5. The Enge split-pole spectrograph, located behind the Si array, was used to monitor the beam energy and purity throughout the runs. The energy loss of ions in the degrader foils and in the ^{232}Th target, as well as the stability and purity of the beam, was measured in the spectrograph. The straggling in the degrader foils gave a maximum energy width for the ^{15}C beam (with the 14.9 mg/cm^2 Au foil) of ~720 keV (FWHM). The relative normalization of the ^{13,14,15}C measurements was achieved by using the elastically scattered particles detected in the four most forward quadrants of the Si detectors ($\theta \sim 35°$) located symmetrically around of the beam.

2.2 Production of the radioactive ^{15}C beam

The ^{15}C beam was produced via the In-Flight Technique [23] by bombarding a cryogenically cooled gas cell filled with deuterium at 1.4 atm with an intense (~100 pnA) ^{14}C beam delivered by the ATLAS accelerator. The ^{15}C ions produced via the d(^{14}C,^{15}C)p reaction were focused with a superconducting solenoid located behind the gas cell and rebunched with a superconducting resonator. The main contaminant in the ^{15}C beam was ^{14}C ions scattered in the production target. An RF sweeper system [24] located midway between the production target and the experimental setup reduced the ^{14}C contamination to 3-28% for the different energies.

Fig. 2 gives a spectrum of time-of-flight vs. magnetic rigidity (Bρ) measured in the focal plane of the spectrograph for the ^{15}C beam attenuated with a 13.2 mg/cm^2 Au foil to an energy of 59.8 MeV. The main peak containing ~72% of the total yield originates from ^{15}C ions, while the group at lower magnetic rigidities results from scattering of the primary ^{14}C beam. Particle identification was obtained using the time-of-flight and the ΔE signals from the focal plane detector. The contaminant ^{14}C^{6+} particles have energies that can be higher than those of ^{15}C^{6+}. Thus, the cross sections for the ^{15}C + ^{232}Th reaction need to be corrected for the contributions from the ^{14}C + ^{232}Th reaction.

The procedure for removing the contribution to the cross section of ^{15}C was to first determine the energy spread of the ^{14}C contaminant given in Fig. 2 , and then correct for the 1/E^2 dependence of the Rutherford cross section using the ^{14}C beam profile. The weighted cross section of this profile was then determined from the extrapolated ^{14}C cross section measured in this experiment. The expected fusion yield from this contaminant beam was removed from the total number of fusion events at this particular beam energy. These corrections to the cross sections are negligible at the two highest energies and increase to 13% for the lowest energy point.

3 Results and Analysis

The experimental fusion-fission cross sections induced by ^{13,14,15}C ions on ^{232}Th are given in Fig. 3 as a function of the center-of-mass energy (top) and as a function of E_{cm}/V_C (bottom), where $V_C = \frac{Z_1 Z_2 e^2}{R}$ is the Coulomb-barrier energy. A radius parameter of 1.44 fm was used for the calculation of V_C. When plotted as a function of E_{cm}/V_C, the cross sections for ^{13,14}C agree within their experimental uncertainties, while the fusion-fission cross section for ^{15}C + ^{232}Th is enhanced at the lowest energies by factors of ~5. This enhancement is similar to that seen in the fusion measurements with the four-neutron halo nucleus ^{8}He on ^{197}Au [25].

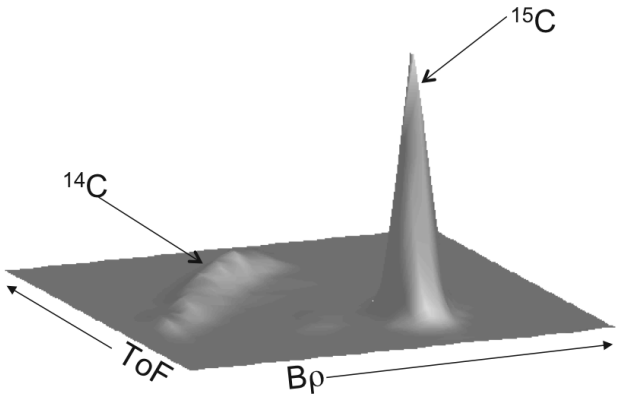

Fig. 2. Spectrum of time-of-flight vs. magnetic rigidity Bρ for a radioactive ^{15}C beam scattered elastically off a ^{232}Th target and detected in the focal plane of the magnetic spectrograph. The beam passed through a 13.2 mg/cm^2 thick Au foil in order to reduce its energy from 73.95 MeV to 59.80 MeV. The contamination of ^{14}C in the ^{15}C beam at this energy was ~12%.

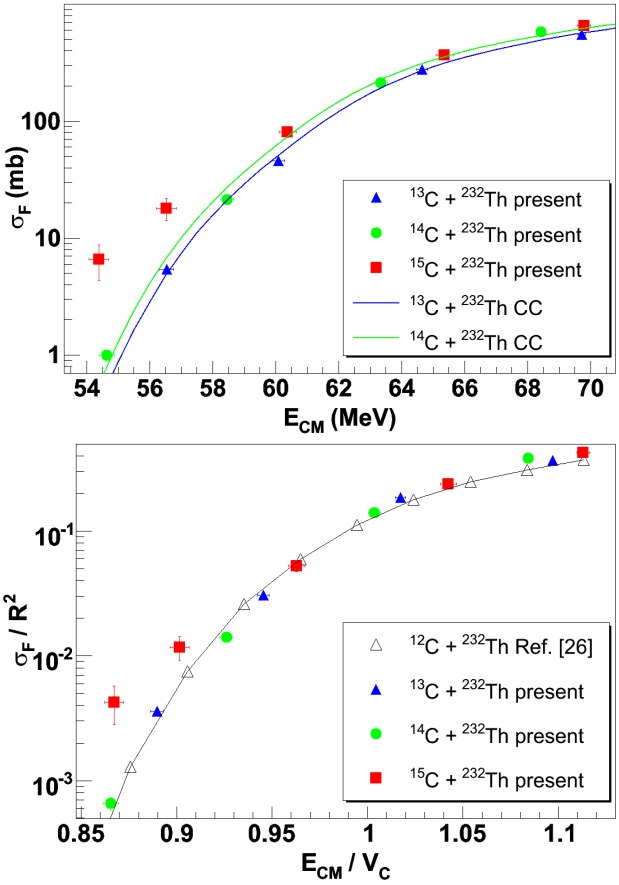

Fig. 3. (top) Cross section of the fusion-fission reactions ^{13,14,15}C + ^{232}Th vs. c.m. energy for the reactions studied in this experiment. If errors bars are not shown, the uncertainties are smaller than the symbols. (bottom) Same as (top) but plotted in reduced coordinates σ/R^2 vs. E_{cm}/V_C. The radii, $R=r_0(A_1^{1/3}+A_2^{1/3})$, were calculated using the radius parameter r_o=1.44 fm. Data for the system ^{12}C + ^{232}Th from Ref. [26] are included. The lines are the result of coupled-channels calculations, see text for details.

3.1 Transfer-induced fission

Due to the low segmentation of the detectors the fusion-fission products could not be distinguished from transfer-induced fission. From experiments with stable beams on ^{232}Th (^{11}B, ^{12}C, ^{13}C and ^{16}O) the maximum contribution from transfer-induced fission was found to be of the order of a few percent relative to the total fusion cross section [22,26,27]. The contribution of transfer-induced fission is therefore expected to be small.

For a quantitative estimate of fission yields from the ^{232}Th(^{15}C,^{14}C) (Q=3.57 MeV) reaction we have used the systematics of neutron transfer obtained from reactions with stable beams in nearby systems [28,29]. The location and the width of the Q-window was calculated with the DWBA program PTOLEMY [30]. In ^{233}Th, only states at excitation energies above 6 MeV can contribute to transfer-induced fission. The total cross section for the (^{15}C,^{14}C) reaction is estimated from systematics to be around 300 mb. Folding the Q-window with the energy-dependent fission probability for ^{233}Th [31], we obtain an upper limit for the transfer-fission yield of about 0.5 mb in the energy range of 54-60 MeV. This is smaller than the fission yields measured in this experiment by a factor of at least 10, meaning the contribution from transfer-induced fission is small for the ^{15}C + ^{232}Th system in the energy range measured in this experiment.

3.2 Coupled-channel calculations

The fusion excitation functions for the systems ^{13,14,15}C + ^{232}Th were compared to the predictions of a coupled-channel treatment performed using the code from Ref. [32]. The coupled-channel calculations include couplings to the quadrupole and octupole excitations. The ion-ion potential is parametrized as a deformed Woods-Saxon potential and curvature corrections are made to first order in the deformation of ^{232}Th.

The results of these calculations for the system ^{13}C + ^{232}Th and ^{14}C + ^{232}Th can be seen in the top of Fig. 3. The calculations for both of these systems reproduce the data well. The CC calculation for the system ^{15}C + ^{232}Th assumes that the valence neutron can be treated as a spectator and the ion-ion potential is the same as that used in the calculation for ^{14}C + ^{232}Th. In fact, the only way the valence neutron appears in the calculation is through the mass of ^{15}C. Therefore, the CC calculation for ^{15}C + ^{232}Th was not included in the figure since the calculation could not be distinguished from that of ^{14}C + ^{232}Th. A comparison to the data as seen in Fig. 3 indicates that at high energies, the fusion data for ^{15}C + ^{232}Th is consistent with the spectator model. However, at low energies (below E_{cm} ~59 MeV), additional effects come into play leading to a strongly enhanced cross section.

4 Summary

The fusion excitation function for the systems ^{14,15}C + ^{232}Th has been measured for the first time. The question

of whether the fusion of nuclei involving weakly bound particles is enhanced or suppressed has been investigated for the halo nucleus ^{15}C. The fusion-fission cross section below the Coulomb barrier shows an enhancement by a factor of 5 compared to that of ^{12,13,14}C. A measurement of the transfer cross sections in ^{15}C + ^{232}Th may help in understanding the effects which lead to the observed enhancement.

Acknowledgements

We would like to thank D. Hinde (ANU) for providing the ^{12}C + ^{232}Th data in tabulated form, and K. L. Jensen (Aarhus University, Denmark) for valuable discussions. We also want to thank the ATLAS operations staff for producing the carbon beams. This work was supported by the U.S. Department of Energy, Office of Nuclear Physics, under Contracts No. DE-AC02-06CH11357 (ANL) and No. DE-FG02-04ER41320 (WMU) and by the NSF JINA Grant No. PHY0822648.

References

1. I. Tanihata et al., Phys. Rev. Lett. **55**, (1985) 2676
2. J. S. Al-Khalili, Lect. Notes Phys. **651**, (2004) 77
3. E. Sauvan et al., Phys. Lett. B **491**, (2000) 1
4. A. Ozawa et al., Nucl. Phys. **A691**, (2001) 599
5. D. Q. Fang et al., Phys. Rev. C **69**, (2004) 034613
6. G. Murillo, S. Sen and S. E. Darden, Nucl. Phys. **A579**, (1994) 125
7. T. Aumann, Nucl. Phys. **A805**, (2008) 198c
8. C. Signorini et al., Nucl. Phys. **A735**, (2004) 329
9. C. Signorini et al., Eur. Phys. J. A **2**, (1998) 227
10. C. Signorini et al., Eur. Phys. J. A **5**, (1999) 7
11. K. E. Rehm et al., Phys. Rev. Lett. **81**, (1998) 3341
12. J. F. Liang and C. Signorini, Int. J. Mod. Phys. E **14**, (2005) 1121
13. W. Loveland, Eur. Phys. J. A **25**, s01, (2005) 233
14. L. F. Canto et al., Phys. Rep. **424**, (2006) 1
15. N. Keeley et al., Prog. Part. Nucl. Phys. **59**, (2007) 579
16. C. Signorini, Nucl. Phys. **A616**, (1997) 262c
17. N. Takigawa and H. Sagawa, Phys. Lett B **265**, (1991) 23
18. M. S. Hussein et al., Phys. Rev. C **46**, (1992) 377
19. M. Ito et al., Phys. Lett. B **637**, (2006) 53
20. N. Keeley and N. Alamanos, Phys. Rev. C **75**, (2007) 054610
21. M. Alcorta et al., Phys. Rev. Lett. **106**, (2011) 172701
22. B. P. Ajith Kumar et al., Phys. Rev. C **72**, (2005) 067601; Phys. Rev. C **73**, (2006) 039901(E)
23. B. Harss et al., Rev. Sci. Instr. **71**, (2000) 380
24. R. C. Pardo et al., in preparation
25. A. Lemasson et al., Phys. Rev. Lett. **103**, (2009) 232701, and references cited therein
26. J. C. Mein et al., Phys. Rev. C **55**, (1997) R995
27. D. M. Nadkarni et al., Phys. Rev. C **59**, (1999) R580
28. K. E. Rehm et al., Phys. Rev. C **42**, (1990) 2497
29. K. E. Rehm, Ann. Rev. Nucl. Part. Sci. **41**, (1991) 429
30. M. H. Macfarlane and S. C. Pieper, Argonne National Laboratory Report No. ANL-76-11 (Rev.1) 1978 (unpublished).
31. B. B. Back et al. Phys. Rev. C **10**, (1974) 1948
32. H. Esbensen and S. Landowne, Nucl. Phys. **A467**, (1987) 136